frontiers | Frontiers in Environmental Science

TYPE Original Research
PUBLISHED 09 December 2024
DOI 10.3389/fenvs.2024.1521144

OPEN ACCESS

EDITED BY
Tao Wang,
Chinese Academy of Sciences (CAS), China

REVIEWED BY
Zhongling Guo,
Hebei Normal University, China
Diwen Cai,
Lingnan Normal University, China

*CORRESPONDENCE
Zhongju Meng,
mengzhongju@126.com

RECEIVED 01 November 2024
ACCEPTED 26 November 2024
PUBLISHED 09 December 2024

CITATION
Meng R, Meng Z, Cai J, Li H, Ren Y and Guo L (2024) The role of typical low vertical lattice sand barriers in regulating the airflow field on wind-eroded surfaces of photovoltaic power plants.
Front. Environ. Sci. 12:1521144.
doi: 10.3389/fenvs.2024.1521144

The role of typical low vertical lattice sand barriers in regulating the airflow field on wind-eroded surfaces of photovoltaic power plants

Ruibing Meng[1,2,3], Zhongju Meng[1,2,3]*, Jiale Cai[1,2,3], Haonian Li[1,2,3], Yu Ren[4] and Lijun Guo[5]

[1]College of Desert Control Science and Engineering, Inner Mongolia Agricultural University, Hohhot, China, [2]Key Laboratory of Aeolian Physics and Desertification Control Engineering from Inner Mongolia Autonomous Region, Inner Mongolia Agricultural University, Hohhot, China, [3]Key Laboratory of Desert Ecosystem Conservation and Restoration, State Forestry and Grassland Administration of China, Inner Mongolia Agricultural University, Hohhot, China, [4]Ordos vocational college of Eco-Environment, Ordos, China, [5]Hangjin Banner Forestry and Grassland Business Development Centre, Ordos, China

Deserts are ideal places to build photovoltaic (PV) power plants, but this plants often face challenges from strong wind and sand activities during the operation and maintenance period, exploring the effects of PV power plant construction on wind disturbances and the control of wind and sand activities by different sand fixation measures is necessary. This study investigated the wind speed outside the PV plant, inside the plant without sand barriers measures (CK), and under three different sand-protecting barriers (gauze sand barriers (GZ), polylactic acid sand barriers (PLA), and grass grid sand barriers (GG)) inside the plant. Though calculated the surface roughness, friction velocity, wind protection effectiveness, and wind turbulence to determined the effectiveness of the barriers by these indexes comprehensively. The results show that: (1) The construction of desert PV power plant can effectively reduce the wind speed. Compared with CK, all three mechanical sand barriers within the plant reduced wind speed. Especially when the height less than 50cm, the GZ sand barriers reduced the wind speeds the most, with an average reduction rate of 101.5%. (2) All three sand barriers increased soil roughness and friction velocity within the power station. (3) At heights below 50cm, the GZ and GG sand barriers have better wind protection effectiveness than PLA sand barriers, while at hights above 100cm, the wind protection effect of PLA and GG sand barriers became less significant or even negligible (4) The wind disturbance caused by the three sand fixation measures increased with wind speed, the comprehensive performance of GZ and PLA sand barriers was superior than that of GG sand barriers and CK.

KEYWORDS

Hobq desert, photovoltaic, mechanical sand barriers, sandstorm, sand break

1 Introduction

The development of new energy sources-photovoltaic (PV) power generation is promising (Shivashankar et al., 2016; Kumar and Saravanan, 2017). The PV systems provide extensive coverage, efficient land utilization, and accessibility to solar resources, making them an attractive energy solution (Hu et al., 2024). Northwest China, characterized with its abundant sunshine hours and intense solar radiation, is particularly well-suited for PV installations, especially in its vast, undeveloped deserts and Gobi landscapes. Moreover, strong government support has facilitated the rapid expansion of large-scale PV power stations in this region (Zhang and He, 2013; Liu et al., 2017).

Current global research on PV power generation primarily focuse on plant siting, panel array configurations, dust accumulation on panels, and vegetation restoration efforts in and around PV sites (Beatty et al., 2017; Said et al., 2018; Colak et al., 2020). However, the construction of PV installations in sandy regions disrupts local geomorphology and wind dynamics, exacerbating soil erosion and negatively impacting the localized microclimate and microtopography (Saidan et al., 2016; Tang et al., 2021; Yue et al., 2021). The erection of PV panels significantly affects wind speed and energy balance within the station, causing sudden changes in surface morphology and resulting in various forms of surface erosion, which can complicate the operation and maintenance of PV power stations (Huang et al., 2018; Al-Dousari et al., 2019).

Wind erosion within PV plants primarily manifests in two forms (Radünz et al., 2021): (1) Hollowing erosion. In sandy regions, PV installations are typically located in mobile sand regions with loose and unstable surface soil. The airflow around the panels creates an acceleration zone, which exposes of the PV system (Wiesinger et al., 2018). (2) Accumulation. Wind-driven sand is transported both beneath and in front of the PV panels, leading to a gradual buildup over time. This accumulation results in uneven topography within the PV station, which poses maintenance challenges and increases costs for the long-term operation of the facility (Middleton et al., 2019).

Currently, research on sand damage control primarily focuses on mechanical sand barriers, which have been extensively utilized in various sand damage scenarios as an efficient means of sand fixation (Qu et al., 2007). These barriers offer excellent protection, are environmentally friendly, and entail low construction costs (Cheng and Xue, 2014). Moreover, mechanical sand barriers effectively reduce near-surface wind speeds and sand-carrying capacity, while simultaneously enhancing soil moisture content and crust thickness within the barriers (Bruno et al., 2018). The implementation of sand barriers alters subsurface properties and increases surface roughness, thus diminishing the intensity of wind erosion (Tuo et al., 2016). This improvement enhances the microenvironment and stability of the sand dune surface, achieving the goal of windbreak and sand fixation, while also creating favorable conditions for subsequent vegetation restoration during construction (Kang et al., 2016). Therefore, laying mechanical sand barriers in the sand-affected areas of PV farms can effectively manage the sand problem between and under the panels (Yang and Qu, 2022; Peng et al., 2023). However, the applicability and limitations of these sand barriers in the specific environment of PV power plants remain unexplored.

Research on how to prevent and control secondary sand damage between panels during operation and maintenance of PV power plants in sandy areas is still in a state of fantasy. Most current studies rely on establishing models, conducting numerical simulations, or performing wind tunnel experiments (Wang C. et al., 2021; Li et al., 2023; Cai et al., 2024; Wan et al., 2024). More field studies are urgently needed to obtain a better understanding of wind erosion patterns and mechanisms in PV stations. The Hobq Desert, characterized by intense wind erosion and sand movement, serves as an ideal location for studying secondary sand damage in PV power stations. Therefore, this study selected the Yili Eco-PV plant in Hobq Desert as the experimental sample site. Three types of mechanical sand barriers (gauze (GZ), Poly Lactic Acid (PLA), and grass grid (GG) sand barriers) were laid in the serious sand damage area in the PV plant. Wind speed measurements were collected in these sand barrier areas, as well as in non-barrier areas within the PV plant and areas outside the PV plant. Field observations of wind velocity and flow field patterns at various heights were conducted to investigate the near-surface wind behavior and the effects of the PV panels and sand barriers. This study seeks to provide theoretical and empirical support for the prevention and control of secondary sand damage in the inter-panel areas of PV power stations situated in sandy regions during their operation and maintenance phases.

2 Materials and methods

2.1 Study area

The study area is located in the Hobq Desert, the seventh largest desert in China, and the administrative region belongs to Hangjin Banner, Ordos City, Inner Mongolia Autonomous Region of China (37°20′-39°50′N, 107°10′-111°45′E (Figure 1). The area has a typical temperate continental climate, characterized by arid conditions and limited rainfall, with an average annual precipitation of 258.30 mm. The annual temperature difference is significant, extreme weather temperature difference of 70°C. The predominant soil type is wind sandy soil, while chestnut calcium soil and meadow soil are found in very limited area. Portions of the region are covered by vegetation, including *Thymus mongolicus Ronniger, Stipa glareosa,* and *Caragana tibetica Kom* (Ouyang et al., 2017; Zhang et al., 2017).

The experimental sample plot is positioned within the Yili 200WP PV Park in Duguitara Township, which was built at the end of 2018. Relative mechanical levelling was carried out prior to the installation of the PV panels. The capacity of the solar PV power station was 200 MW-p and covered an area of 6.67 km^2. The study area was windy, with frequent sand and wind disasters. The mean annual wind speed was 3.78 m/s, with a maximum wind speed that reached 31 m/s. It had mean annual 24.8 days of gale-force winds, 102 days of sand lifting, and 20 days of sandstorms. Sand and wind activities were primarily influenced by northwesterly and westerly winds. Under the influence of these winds, the ground surface remained dry, vegetation was sparse, and sanding occurred frequently. Notably, wind speeds between 6.00 m/s and 8.00 m/s occurred most often, followed by speeds between 8.00 m/s and 10.00 m/s, accounting for 92%–95% of all sanding winds (Figure 2).

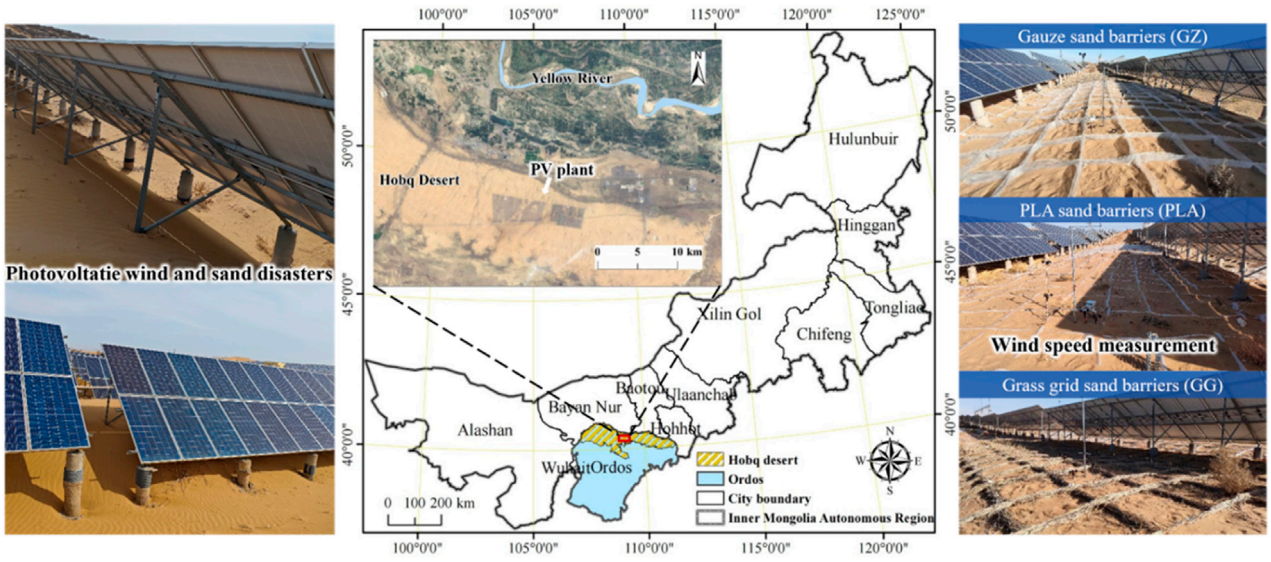

FIGURE 1
Overview map of the study area.

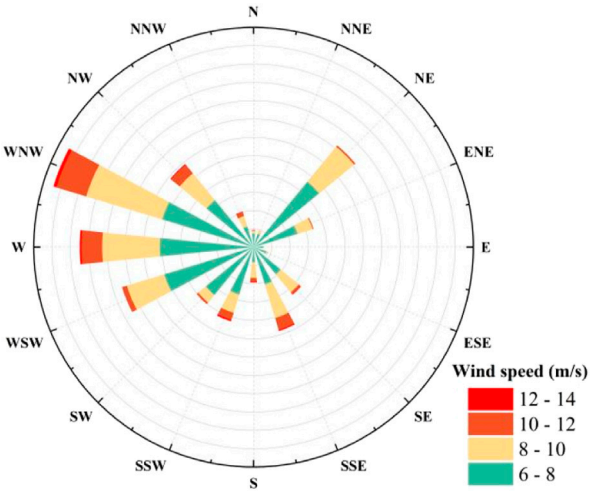

FIGURE 2
Rose map of sandy winds from the year.

2.2 Sample layouts

The sand barriers for this experiment were laid on the inside of the Yili PV plant in the Hobq Desert. Thay were aligned north-south, with the PV panels tilted at the optimal tilt angle (37°). Sand barriers were deployed in April 2023, with the three types of sand barriers between the boards as the study and bare sand at the same site as a control (CK) (Figure 1). Three lattice sand barriers (1 m × 1 m) were deployed (Table 1). The first type is a gauze sand barriers (GZ), with a height of 15–20 cm, which is a type of permeable sand barrier developed in recent years, made of polyethylene, with high resistance to aging. The second type is the PLA sand barriers (PLA). Created by filling *in situ* sand into a columnar bag crafted from PLA, this barrier stands at a height of 7–9 cm. Its unique feature lies in its biodegradability and aging resistance, offering a sustainable method of sand treatment. The third type is the grass grid sand barriers (GG), with a height of 15–20 cm, which is the most common type of sand barrier in sand control and prevention, inexpensive and made of local wheat grass and straw.

2.3 Measurement methods

The sand barriers in the test area were laid in April 2023, and wind speed observations were made on the underlay of the laid sand barriers immediately after they were laid. Observations were made at heights of 10, 20, 50, 100, and 200 cm, and wind observations at each height were made above the center of the baffle, with three sets of anemometers set up in each sample plot (Figure 3). The interval between wind speed recordings was 2 s. The second wind-sand observation was made on a typical spring windy day in April 2024, and the wind direction was the same as that of the 2023 observation. At this time, after a year of erosion of the sand barriers, the curved surface morphology of the barriers has reached a stable stage, and the wind speed of the sand barriers is measured again (the wind speed measurement method is the same as that of 2023) to find out the changes in the wind protection benefits. In this experiment, a small weather station, HOBO-U30, produced by Onset Company of the United States, collected wind speed.

Wind speed profile equation: In this study, Platt-von Kamen's law of logarithmic distribution of wind speed is used to describe the wind speed profile Equation 1 as (Wiggs, 1993):

$$U_Z = \frac{U_\star}{K} \ln \frac{Z}{Z_0} \quad (1)$$

TABLE 1 Detailed information of three types of sand barriers.

Sand barrier type	Name	Height (cm)	Material	Characteristics
Gauze sand barriers	GZ	15–20	High density polyethylene	Permeable, high resistance to aging
PLA sand barriers	PLA	7–9	PLA (Polylactic Acid)	Biodegradable, aging-resistant, eco-friendly
Grass grid sand barriers	GG	15–20	Wheat grass, straw	Low-cost, commonly used in sand control

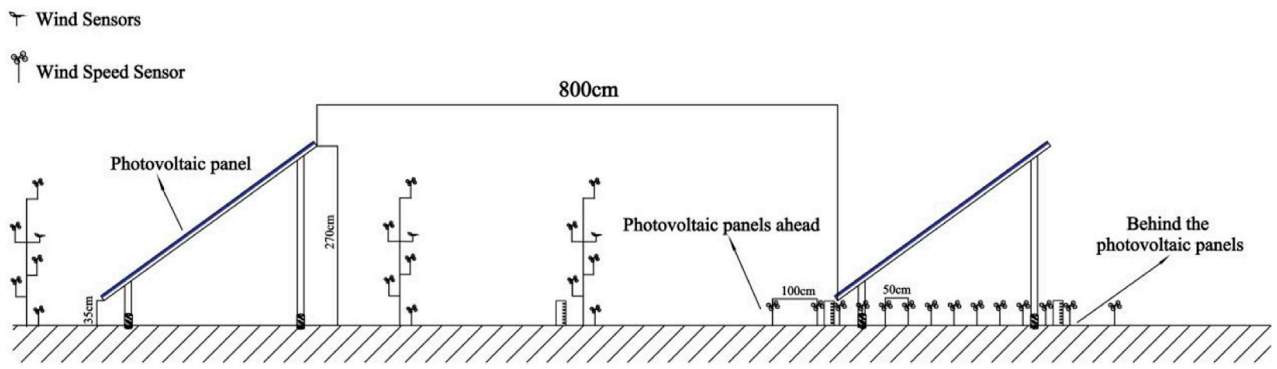

FIGURE 3
Field configurations used to test the wind flow field characteristics and sand transport.

Where: U_z on behalf of the Z height of the average wind speed (m/s); U* on behalf of the friction velocity (m/s); Z for the wind speed profile at a point on the vertical height from the ground (cm); Z_0 for the aerodynamic roughness (cm); K for the Carmen's constant, the value of 0.4.

Aerodynamic roughness and friction velocity: In this study, the logarithmic contour fitting method was used to calculate. The wind speeds were measured at five heights (0.1, 0.2, 0.5, 1 and 2 m), and the wind speed contour equation was obtained by least squares regression (Sharratt and Feng, 2009). The formula is as follows:

$$U_Z = a + b \ln Z \tag{2}$$

Where a,b are regression coefficients. The surface roughness can be found by making = 0.

$$Z_0 = exp(-a/b) \tag{3}$$

Calculated from Equations 2, 3, the Equation 4 for the calculation of the friction velocity is given by:

$$U* = Kb \tag{4}$$

The wind protection effectiveness is calculated as Equation 5 (Shi et al., 2020):

$$F = \frac{V_0 - V_{sb}}{V_0} \times 100\% \tag{5}$$

Where F is the windproof efficiency of the sand barriers (%), V_0 and V_{sb} represents the wind speed of bare sand at the same height and the wind speed after laying various sand barriers (m/s), respectively.

Degree of wind disturbance: Wind speed data at 10 and 20 cm heights near the surface of each underlay were investigated to understand the effect of sand barriers on the degree of wind perturbation, Equation 7 is calculated through Equation 6 as follows:

$$S = \sqrt{\frac{\sum (V - \bar{V})^2}{N - 1}} \tag{6}$$

$$D = S/\bar{V} \tag{7}$$

Where V is a set of wind speed data (V_1, V_2, V_3,) observed in a certain period of time (m/s); $\bar{V}$ is the average wind speed in that period (m/s); N is the number of the set of wind speed data; S is the standard deviation; D is the degree of wind disturbance.

2.4 Processing and analysing data

Excel 2021 and Origin 2023 software were used to collate and analyze the data and graphical work. The data were analyzed by one-way ANOVA using SPSS 25 software, and the data were presented as mean ± standard value and LSD multiple tests.

3 Result

3.1 Wind speed profile for different sand fixation measures at various wind speeds

The wind speed profile, alternatively termed as mean wind speed gradient or wind profile, represents the distribution curve of wind speed with height, one of the critical indicators of wind speed measurement. It is affected by the combined effects of factors such as topography, surface structural stability and weather

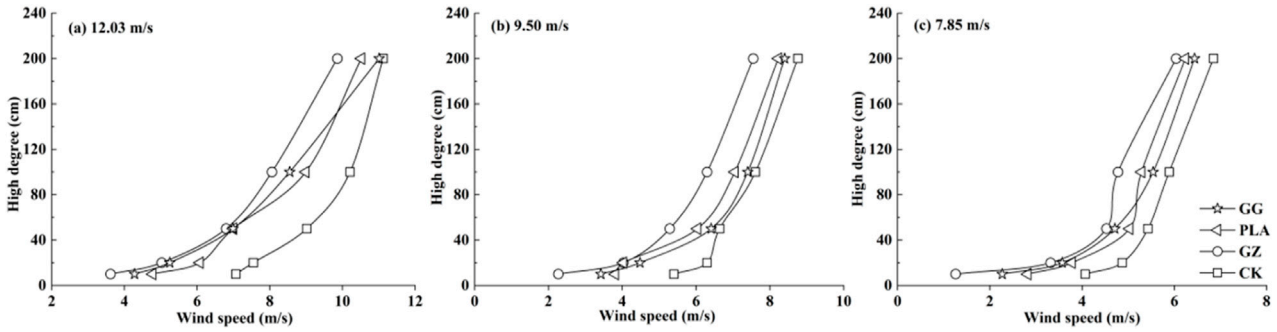

FIGURE 4
Wind speed profiles at different wind speeds: **(A)** 12.03 m/s, **(B)** 9.50 m/s, **(C)** 7.85 m/s.

conditions In this study, laying sand barriers in the sample plots effectively changed the ground surface's micro-morphology, resulting in wind speed profiles that differed from the original wind speed profiles. As illustrated in Figure 4, laying all three types of sand barriers in the PV plant can effectively reduce the wind speed in the wilderness, and this reduction is especially obvious at the heights of 10 cm and 20 cm. The wind speed profile of CK has a "J" shape, in contrast, the wind speed profile of GG sand barriers is similar to that of CK, but shows a difference below 50 cm, and the difference is because the wind blocking effect of the sand barriers on the near-surface in the 10–50 cm range, resulting in the wind speed profiles of GG sand barriers tend to flatten out in this height range. However, the wind speed profiles of GZ and PLA sand barriers showed slightly variable characteristics at wind speeds of 12.03 m/s and 7.85 m/s. At heights between 20 and 50 cm, the wind speed decay increases, leading a significant increase in slope at this location. Above 50 cm, it returns to the same rate of increase as the wind speed in the open field. Combining these properties, the GG sand barriers showed relatively small changes in the wind speed profile, while the GZ and PLA sand barriers show significant attenuation in the near-surface region (below 50 cm) after laying. This phenomenon attributed to the stabilisation of the surface morphology after the sand barriers were deployed, and the characteristics of the sand barriers themselves. The GZ sand barriers is a permeable sand barrier, which can effectively attenuate the effect of near-surface wind speed. Meanwhile, the PLA sand barriers are solid barriers that gradually form a stable concave structure over time, which positively regulate the wind speed distribution and flow field properties.

3.2 Soil surface roughness and friction velocity at different wind speeds

Table 2 illustrates the wind speed profile regression of the three sand barriers at different wind speed. The good fit ($R^2 > 0.938$) of the wind speed profile data provided confidence in estimating aerodynamic roughness and friction velocity values. The laying of sand barriers changes the surface micro-morphology. The form and degree of undulation can be attributed to the scale range of roughness, which is an essential indicator in the physics of wind and sand and plays an indispensable role in measuring the effectiveness of sand control. This is typically expressed in terms of zero-plane displacement height, the friction velocity also plays a vital role in determining surface sand uplift. As shown in Figure 5, the aerodynamic roughness of all three mechanical sand fixation measures (GZ, PLA, and GG) was significantly higher than that of CK. In particular, the aerodynamic roughness within the sand barriers increased at 12.03 m/s compared with the other two wind speeds; the aerodynamic roughness within all three sand barriers at different wind speeds showed GZ sand barriers with GG sand barriers higher than PLA sand barriers. Comparing the aerodynamic roughness of GZ sand barriers under the three wind speeds individually, we find that the aerodynamic roughness increases with the decrease of wind speed; PLA sand barriers reaches the highest value at 9.50 m/s wind speed, and the aerodynamic roughness pattern of GG sand barriers is the same as that of GZ sand barriers. In summary, all three measures improve the aerodynamic roughness of the ground surface in the PV plant, and each measure has certain advantages under different wind speeds.

A pattern can be found that the wind's friction velocity reduces with decreasing wind speed, with or without the sand barrier measure, and the CK friction velocity is much lower than the three measures, regardless of the type of wind speed (Figure 6). At wind speeds up to 12.03 m/s, the three sand barriers showed an increase of 44.33%, 32.82%, and 54.91% in friction velocity compared to CK, and at 9.50 m/s, the three sand barriers showed an increase of 61.24%, 50.00% and 62.68% in friction velocity, respectively; at a wind speed of 7.85 m/s, the friction velocity of the three types of sand barriers increased by 68.60%, 28.20%, and 57.56%, respectively. The GZ sand barriers, by their unique material composition, can effectively change the wind velocity and flow field, which will also significantly impact the various indicators of the ground surface. As a new type of biodegradable sand barrier, PLA sand barriers can do "sand to cure sand" in the wind, and sand performance is excellent; GG sand barriers, as traditional sand fixation measures, wind and sand performance sound.

3.3 Wind protection effectiveness of different sand barriers

Windproof efficiency can effectively reflect the windproof ability of sand barriers; the larger the value of windproof efficiency, the stronger the sand barrier's windproof and sand-fixing ability is, and

TABLE 2 Wind speed profile regression equation.

Wind speed	Type	Wind speed profile regression equation
12.03 m/s	CK	u = 3.260ln(z)+3.580 R^2 = 0.983
	GZ	u = 4.720ln(z)-1.007 R^2 = 0.976
	PLA	u = 4.328ln(z)+0.289 R^2 = 0.966
	GG	u = 5.050ln(z)-1.170 R^2 = 0.962
9.50 m/s	CK	u = 1.045ln(z)+2.947 R^2 = 0.938
	GZ	u = 1.685ln(z)-1.352 R^2 = 0.985
	PLA	u = 1.567ln(z)-0.157 R^2 = 0.964
	GG	u = 1.701ln(z)-0.480 R^2 = 0.983
7.85 m/s	CK	u = 0.861ln(z)+2.132 R^2 = 0.970
	GZ	u = 1.449ln(z)-1.555 R^2 = 0.993
	PLA	u = 1.102ln(z)+0.420 R^2 = 0.971
	GG	u = 1.356ln(z)-0.678 R^2 = 0.990

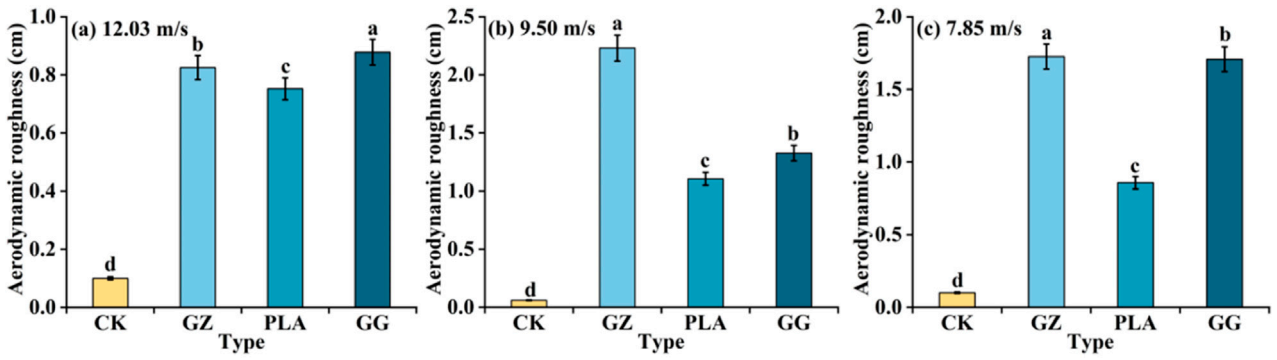

FIGURE 5
Aerodynamic roughness at different wind speeds: **(A)** 12.03 m/s, **(B)** 9.50 m/s, **(C)** 7.85 m/s.

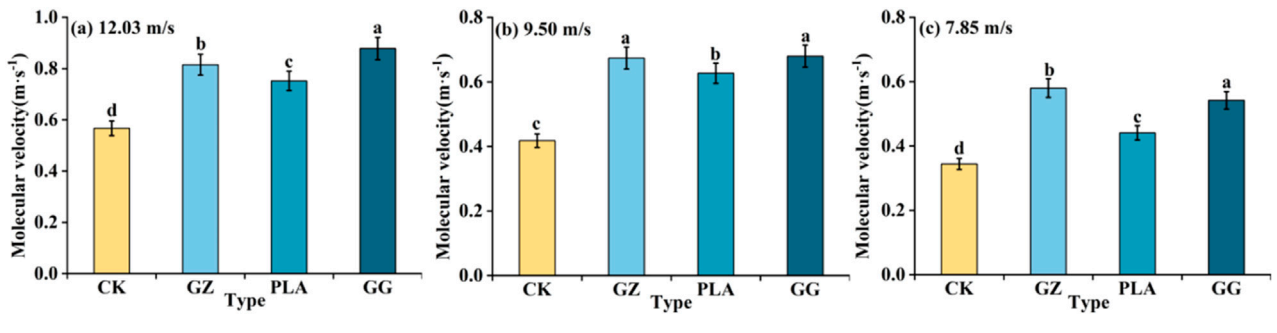

FIGURE 6
Soil friction velocity at different wind speeds: **(A)** 12.03 m/s; **(B)** 9.50 m/s; **(C)** 7.85 m/s.

the stronger the ability to cut down the wind. As shown in Figure 7, all three mechanical sand barriers provide reasonable wind control in the PV station, and have the best windproof effect at 10cm and 20 cm near the ground surface. Among them, the GZ sand barriers were the most effective, which is nearly 50% at 10cm and 33% at 20 cm. The GG sand barriers were the second most effective, and the PLA sand barriers were less effective than the other two types. The wind protection effectiveness of the three sand barriers decreased

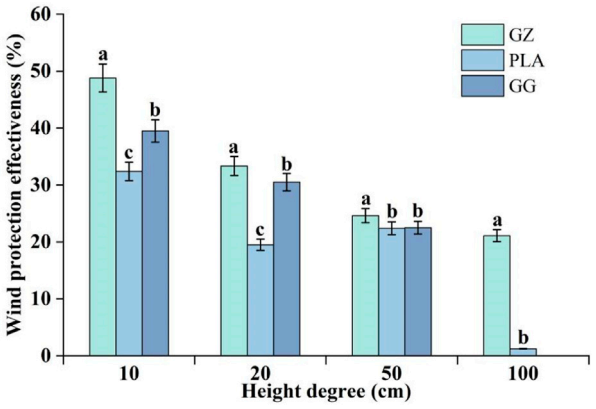

FIGURE 7
Wind protection effectiveness of three types of sand barriers.

with the increasing vertical height and was lowest at 100 cm, while the weakening ability of PLA and GG sand barriers for wind was almost negligible.

3.4 The degree of disturbance of different sand barriers to the wind

As shown in Figure 8, at 10 cm near the surface, all three mechanical sand barriers and CK became more extensive as the wind speed increased. There was a significant difference ($p < 0.05$) between each measure and CK, except for PLA sand barriers, which was insignificant ($p > 0.05$) between PLA sand barriers and CK at 9.50 m/s. When the wind speed reaches 7.85 m/s, the GZ sand barriers disturbance is the lowest. When the wind speed reaches 12.03 m/s, the GG sand barriers disturbance is the lowest compared to CK, which is 3% and 51% lower, respectively. The perturbation of wind at 10 cm near the surface was lower than that of CK for all three sand barriers. It can be seen that the three sand barriers effectively suppress wind speed.

At 20 cm near the surface, the difference between CK and the three sand barriers was significant ($p < 0.05$). When the wind speed was 7.85 m/s, and the disturbance of CK was higher than that of the three sand barriers. At wind speeds up to 9.50 m/s, CK was still more perturbing to the wind than the three sand barriers, but at this point, there was already a non-significant difference between CK and GZ sand barriers ($p > 0.05$). When the wind speed reaches 12.03 m/s, the perturbation degree of GZ sand barriers is higher than that of CK, PLA and GG sand barriers, and the difference between them is significant. This is because GZ sand barriers is a flexible sand barrier and when the wind speed reaches a certain intensity, GZ sand barriers will bend and swing with the wind, hence the degree of wind disturbance increased significantly.

4 Discussion

This study measured wind speed under three distinct conditions: the open field outside the PV plant, bare sandy land within the PV plant, and three types of sand barriers (GZ PLA, and GG). The results revealed that the construction of PV plant in a desert area significantly reduces the wind speed in the open fields, thereby confirming the positive role of PV plants in mitigating wind disturbances. Furthermore, through calculatiions of surface roughness, friction velocity, wind protection effectiveness, and the degree of wind disturbance, we found that all three types of sand barriers successfully decreased wind speeds on bare sand, altered wind flow patterns, increased surface roughness and friction velocity, and contributed to mitigating wind erosion. Among these, the GZ sand barrier exhibited the highest overall effectiveness, outperforming the other two barriers in most indicators, particularly in terms of reducing wind speeds near the

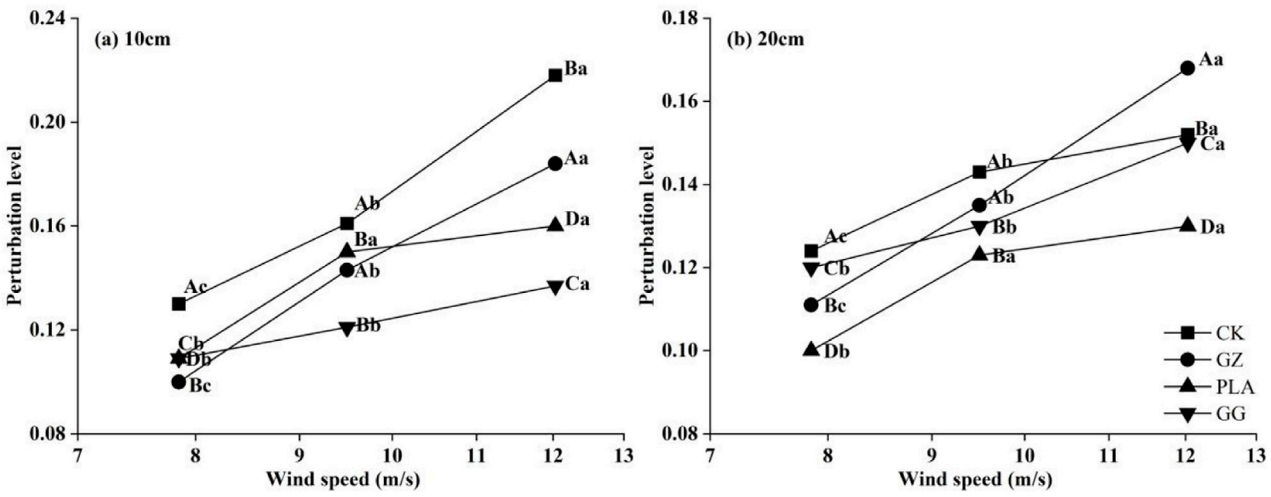

FIGURE 8
Degree of wind disturbance for various types of sand barriers: **(A)** 10 cm near surface; **(B)** 20 cm near surface. Note: Different capital letters indicate significant ($P < 0.05$) differences in wind perturbation for different sand barriers at the same wind speed, and different lower case letters indicate significant ($P < 0.05$) differences in wind perturbation for the same sand barrier type at different wind speeds.

surface and providing stronger windbreak effect. The superior performance of GZ sand barriers in increasing friction velocity highlights its potential for effectively stabilizing sand and enhancing soil retention (Radünz et al., 2021). In alignment with the findings of Luo et al. (2023), vertical mesh barrier can effectively reduce near-surface wind speed and sediment transport, and the effectiveness of grid-shaped sand barrier exceeds that of strip-type barriers. Considering the challenges posed by variable wind speeds and directions in desert regions where PV plants are located, we recommend prioritizing the use of grid-shaped GZ sand barriers when implementing sand protection measures around power plants. Additionally, Dang et al. (2023), further confirmed the findings of this study by investigating the wind protection capabilities of different shapes of GZ sand barriers.

Although the GZ sand barriers excel in numerous aspects, is it infallible? Is it ideally suited for sand fixation measures in PV power plants? In contrast, GZ sand barriers, made of high-density polyethylene, suffer from drawbacks such as non-biodegradability, high costs, and potential damage over time during installation, posing environmental threats that contradict their intended purpose of environmental protection (Zhang et al., 2024). On the other hand, GG sand barriers offers advantages such as low price, rapid installation, and the use of locally sourced materials. It enhances the ability of the dune system to intercept sand and dust, promotes the accumulation of soil organic matter and nutrients, and improves the role of the dune surface as soil formation (Luo et al., 2019). Straw checkerboard sand barriers increased the content of silt and clay particles, thereby refining soil texture (Luo et al., 2023), which is a necessary prerequisites for the invasion and settlement of herbaceous plants in desert ecosystems (Wang R. et al., 2021). When the straw checkerboard stabilizes dunes to establish sand-fixing vegetation, plant species richness, herbaceous cover, dust deposition, and soil physicochemical properties significantly differ from sandy areas without measures (Wang et al., 2020). However, long-term field observations indicate that the service life of straw checkerboard sand barriers is relatively short, and their wind prevention and sand fixation effects gradually weaken over time, posing potential risks to the long-term stable operation of PV plants (Li et al., 2006). The PLA, made of polylactic acid, has attracted attention due to its superior biodegradability. Studies have shown that it performs well in sand consolidation, with an effective working life of 10–15 years (Yang et al., 2023). Nevertheless, its sand fixation effectiveness diminishes over time, necessitating consideration of both durability and environmental friendliness. Notably, the PLA only generates CO_2 and H_2O during decomposition, which will not pollute the environment. Additionally, Xie et al. (2020) found that PLA sand barriers showed a more significant trend in reducing fine-grained sediments than traditional bare sand barriers, especially on the surface. The high water retention capacity of PLA materials can also effectively retain water in arid desert environments, which is particularly favourable for the subsequent vegetation reconstruction in PV plants (Messin et al., 2020).

Each type of sand barrier has its unique advantages and corresponding limitations (Han et al., 2003; Wang et al., 2023). Based on our findings and discussions, we propose a combination method to address these limitations: GZ sand barriers can be deployed in high-wind zones, such as areas beneath PV panels, to maximize wind protection. PLA sand barriers can be utilized in moderate wind regions to improve soil moisture retention and support vegetation growth. GG sand barriers, due to their low cost and ease of installation, can be laid in low-wind areas to expand sand fixation coverage. This integrated strategy optimizes the strengths of each barrier type while minimizing their respective weaknesses. Previous studies (Dang et al., 2015) has showed that combining different barriers can improve sand fixation benefits, supporting the feasibility of this approach in desert PV power stations. Future research should focus on the precise configuration, spacing, and cost-benefit analysis of these combinations to maximize their efficiency and sustainability in real-world applications.

5 Conclusion

Based on our comprehensive analysis of wind speed, surface roughness, and friction velocity both outside and inside the PV plant, along with the wind protection performance of the sand barriers, we obtained the following key findings:

(1) The PV plant significantly reduced wind speeds in the surrounding wilderness, demonstrating its potential to mitigate wind disturbances outside the plant.
(2) While reducing the wind speed in the wilderness, the three types of sand barriers laid in the PV power station successfully reduced the wind speed in the bare sandy area of the station and improved the friction velocity; the wind protection effectiveness was shown as GZ>GG>PLA.
(3) Among the evaluated sand barriers,the GZ sand barriers demonstrated the most superior wind protection performance, followed by the GG and PLA sand barriers. As wind speeds escalated at heights of 10 cm and 20 cm near the surface, the disturbance effect of each sand barrier intensified.
(4) The findings suggest that a strategic combination of sand barriers can optimize their complementary advantages. GZ sand barriers can be placed in areas with strong wind to enhance windbreak effects, PLA sand barriers in areas necessitating environmental protection and vegetation restoration, and GG sand barriers in regions with weaker winds to bolster soil stability.

Data availability statement

The original contributions presented in the study are included in the article/supplementary material, further inquiries can be directed to the corresponding author.

Author contributions

RM: Conceptualization, Data curation, Investigation, Methodology, Visualization, Writing–original draft. ZM: Conceptualization, Data curation, Funding acquisition,

Methodology, Visualization, Writing–review and editing. JC: Conceptualization, Methodology, Supervision, Writing–original draft. HL: Methodology, Writing–review and editing. YR: Methodology, Writing–review and editing. LG: Conceptualization, Funding acquisition, Writing–review and editing.

Funding

The author(s) declare that financial support was received for the research, authorship, and/or publication of this article. This research was supported by the Major Science and Technology Project of Ordos City (2022EEDSKJZDZX020-4), Open Project of Inner Mongolia Autonomous Region Forestry Science Research Institute: Mutual Feedback Mechanism between Photovoltaic Power Field and Environment in Sandy Area (KF2024ZD02), Basic Research Funds for Universities-Innovation Team Building–Desert Ecosystem Protection and Restoration Innovation Team (BR22-13-03).

Conflict of interest

The authors declare that the research was conducted in the absence of any commercial or financial relationships that could be construed as a potential conflict of interest.

Generative AI statement

The author(s) declare that no Generative AI was used in the creation of this manuscript.

Publisher's note

References

Al-Dousari, A., Al-Nassar, W., Al-Hemoud, A., Alsaleh, A., Ramadan, A., Al-Dousari, N., et al. (2019). Solar and wind energy: challenges and solutions in desert regions. *Energy* 176, 184–194. doi:10.1016/j.energy.2019.03.180

Beatty, B., Macknick, J., McCall, J., Braus, G., and Buckner, D. (2017). Native vegetation performance under a solar PV array at the national wind technology center. *Tech. Rep.* doi:10.2172/1357887

Bruno, L., Coste, N., Fransos, D., Lo Giudice, A., Preziosi, L., and Raffaele, L. (2018). Shield for sand: an innovative barrier for windblown sand mitigation. *ENG* 12, 237–246. doi:10.2174/1872212112666180309151818

Cai, J., Meng, Z., Meng, R., Li, H., Chen, X., Ren, X., et al. (2024). Exploring a path of vegetation restoration best suited for a photovoltaic plant in the hobq desert. *Front. Environ. Sci.* 12, 1380421. doi:10.3389/fenvs.2024.1380421

Cheng, J., and Xue, C. (2014). The sand-damage–prevention engineering system for the railway in the desert region of the qinghai-tibet plateau. *J. Wind Eng. Industrial Aerodynamics* 125, 30–37. doi:10.1016/j.jweia.2013.11.016

Colak, H. E., Memisoglu, T., and Gercek, Y. (2020). Optimal site selection for solar photovoltaic (PV) power plants using GIS and AHP: a case study of malatya province, Turkey. *Renew. Energy* 149, 565–576. doi:10.1016/j.renene.2019.12.078

Dang, X., Chi, X., Tang, G., Meng, Z., Huang, H., Zhai, B., et al. (2023). Numerical study on wind profiles change trend of upright reticulation barriers under different configuration models. *Front. Environ. Sci.* 11, 1159977. doi:10.3389/fenvs.2023.1159977

Dang, X., Gao, Y., and Yu, Y. (2015). Windproof efficiency with new biodegradable PLA sand barrier and traditional straw sand barrier. *J. Beijing For. Univ.* 37 (3), 118–125. doi:10.13332/j.1000-1522.20140245

Han, Z., Wang, T., Sun, Q., Dong, Z., and Wang, X. (2003). Sand harm in taklimakan desert highway and sand control. *J. Geogr. Sci.* 13, 45–53. doi:10.1007/BF02873146

Hu, J., Yang, P., Li, Q., Wang, M., Feng, J., Gao, Z., et al. (2024). Evaluation of groundwater vulnerability of yishu river basin based on DRASTIC-GIS model. *Water* 16, 429. doi:10.3390/w16030429

Huang, B., Li, Z., Zhao, Z., Wu, H., Zhou, H., and Cong, S. (2018). Near-ground impurity-free wind and wind-driven sand of photovoltaic power stations in a desert area. *J. Wind Eng. Industrial Aerodynamics* 179, 483–502. doi:10.1016/j.jweia.2018.06.017

Kang, L., Zou, X., Zhao, G., Zhang, C., and Cheng, H. (2016). Wind tunnel investigation of horizontal and vertical sand fluxes of ascending and descending sand particles in aeolian sand transport. *Earth Surf. Process. Landf.* 41, 1647–1657. doi:10.1002/esp.3935

Kumar, K. P., and Saravanan, B. (2017). Recent techniques to model uncertainties in power generation from renewable energy sources and loads in microgrids – a review. *Renew. Sustain. Energy Rev.* 71, 348–358. doi:10.1016/j.rser.2016.12.063

Li, P., Luo, Y., He, Z., Zheng, J., Xia, X., Liao, Z., et al. (2023). A comparative study of the effects of photovoltaic power plants in desert and lake on the microclimate. *Energy Rep.* 10, 2128–2137. doi:10.1016/j.egyr.2023.08.064

Li, X. R., Xiao, H. L., He, M. Z., and Zhang, J. G. (2006). Sand barriers of straw checkerboards for habitat restoration in extremely arid desert regions. *Ecol. Eng.* 28, 149–157. doi:10.1016/j.ecoleng.2006.05.020

Liu, J., Xu, F., and Lin, S. (2017). Site selection of photovoltaic power plants in a value chain based on grey cumulative prospect theory for sustainability: a case study in northwest China. *J. Clean. Prod.* 148, 386–397. doi:10.1016/j.jclepro.2017.02.012

Luo, J., Deng, D., Zhang, L., Zhu, X., Chen, D., and Zhou, J. (2019). Soil and vegetation conditions changes following the different sand dune restoration measures on the zoige plateau. *PLoS ONE* 14, e0216975. doi:10.1371/journal.pone.0216975

Luo, X., Li, J., Tang, G., Li, Y., Wang, R., Han, Z., et al. (2023). Interference effect of configuration parameters of vertical sand-obstacles on near-surface sand transport. *Front. Environ. Sci.* 11, 1215890. doi:10.3389/fenvs.2023.1215890

Messin, T., Marais, S., Follain, N., Guinault, A., Gaucher, V., Delpouve, N., et al. (2020). Biodegradable PLA/PBS multinanolayer membrane with enhanced barrier performances. *J. Membr. Sci.* 598, 117777. doi:10.1016/j.memsci.2019.117777

Middleton, N., Tozer, P., and Tozer, B. (2019). Sand and dust storms: underrated natural hazards. *Disasters* 43, 390–409. doi:10.1111/disa.12320

Ouyang, H., Lan, S., Yang, H., and Hu, C. (2017). Mechanism of biocrusts boosting and utilizing non-rainfall water in hobq desert of China. *Appl. Soil Ecol.* 120, 70–80. doi:10.1016/j.apsoil.2017.07.024

Peng, H., Jin, A., Zhang, S., and Zheng, B. (2023). Numerical simulation and parameter optimization of a new reed–nylon net combined sand fence. *Sustainability* 15, 13920. doi:10.3390/su151813920

Qu, J., Zu, R., Zhang, K., and Fang, H. (2007). Field observations on the protective effect of semi-buried checkerboard sand barriers. *Geomorphology* 88, 193–200. doi:10.1016/j.geomorph.2006.11.006

Radünz, W. C., Sakagami, Y., Haas, R., Petry, A. P., Passos, J. C., Miqueletti, M., et al. (2021). Influence of atmospheric stability on wind farm performance in complex terrain. *Appl. Energy* 282, 116149. doi:10.1016/j.apenergy.2020.116149

Said, S. A. M., Hassan, G., Walwil, H. M., and Al-Aqeeli, N. (2018). The effect of environmental factors and dust accumulation on photovoltaic modules and dust-accumulation mitigation strategies. *Renew. Sustain. Energy Rev.* 82, 743–760. doi:10.1016/j.rser.2017.09.042

Saidan, M., Albaali, A. G., Alasis, E., and Kaldellis, J. K. (2016). Experimental study on the effect of dust deposition on solar photovoltaic panels in desert environment. *Renew. Energy* 92, 499–505. doi:10.1016/j.renene.2016.02.031

Sharratt, B., and Feng, G. (2009). Friction velocity and aerodynamic roughness of conventional and undercutter tillage within the columbia plateau, USA. *Soil Tillage Res.* 105, 236–241. doi:10.1016/j.still.2009.08.004

Shi, T., Meng, Z., Cui, X., Dang, X., Tang, G., and Jia, R. (2020). Wind-prevention and Sand-fixing benefits of reed-sand barrier at photovoltaic plant in Hobq desert. *Bull. Soil Water Conserv.* 40, 166–171. doi:10.13961/j.cnki.stbctb.2020.05.025

Shivashankar, S., Mekhilef, S., Mokhlis, H., and Karimi, M. (2016). Mitigating methods of power fluctuation of photovoltaic (PV) sources – a review. *Renew. Sustain. Energy Rev.* 59, 1170–1184. doi:10.1016/j.rser.2016.01.059

Tang, G., Meng, Z., Gao, Y., and Dang, X. (2021). Impact of utility-scale solar photovoltaic array on the aeolian sediment transport in hobq desert, China. *J. Arid. Land* 13, 274–289. doi:10.1007/s40333-021-0096-y

Tuo, D., Xu, M., Gao, L., Zhang, S., and Liu, S. (2016). Changed surface roughness by wind erosion accelerates water erosion. *J. Soils Sediments* 16, 105–114. doi:10.1007/s11368-015-1171-x

Wan, L., Zhao, L., Xu, W., Guo, F., and Jiang, X. (2024). Dust deposition on the photovoltaic panel: a comprehensive survey on mechanisms, effects, mathematical modeling, cleaning methods, and monitoring systems. *Sol. Energy* 268, 112300. doi:10.1016/j.solener.2023.112300

Wang, C., Hill, R. L., Bu, C., Li, B., Yuan, F., Yang, Y., et al. (2021a). Evaluation of wind erosion control practices at a photovoltaic power station within a sandy area of northwest, China. *Land Degrad. Dev.* 32, 1854–1872. doi:10.1002/ldr.3839

Wang, F., Liu, S., Jiang, Y., and Duan, W. (2023). Research on the effect of sand barriers on highways in desert areas on sand control. *Sustainability* 15, 13906. doi:10.3390/su151813906

Wang, R., Gao, Y., Dang, X., Yang, X., Liang, Y., and Zhao, C. (2021b). Microstructure and biodegradation of long-established salix psammophila sand barriers on sand dunes. *Environ. Technol. and Innovation* 21, 101366. doi:10.1016/j.eti.2021.101366

Wang, T., Qu, J., and Niu, Q. (2020). Comparative study of the shelter efficacy of straw checkerboard barriers and rocky checkerboard barriers in a wind tunnel. *Aeolian Res.* 43, 100575. doi:10.1016/j.aeolia.2020.100575

Wiesinger, F., Sutter, F., Wolfertstetter, F., Hanrieder, N., Fernández-García, A., Pitz-Paal, R., et al. (2018). Assessment of the erosion risk of sandstorms on solar energy technology at two sites in morocco. *Sol. Energy* 162, 217–228. doi:10.1016/j.solener.2018.01.004

Wiggs, G. F. S. (1993). Desert dune dynamics and the evaluation of shear velocity: an integrated approach. *SP* 72, 37–46. doi:10.1144/GSL.SP.1993.072.01.05

Xie, Y., Dang, X., Zhou, Y., Hou, Z., Li, X., Jiang, H., et al. (2020). Using sediment grain size characteristics to assess effectiveness of mechanical sand barriers in reducing erosion. *Sci. Rep.* 10, 14009. doi:10.1038/s41598-020-71053-3

Yang, S., and Qu, Z. (2022). Cost analysis of sand barriers in desertified regions based on the land grid division model. *J. Arid. Land* 14, 978–992. doi:10.1007/s40333-022-0072-2

Yang, W., Du, Y., and Liu, B. (2023). Novel environmentally friendly covalent organic framework/polylactic acid composite material with high chemical stability for sand-control material. *Polymers* 15, 1659. doi:10.3390/polym15071659

Yue, S., Wu, W., Zhou, X., Ren, L., and Wang, J. (2021). The influence of photovoltaic panels on soil temperature in the gonghe desert area. *Environ. Eng. Sci.* 38, 910–920. doi:10.1089/ees.2021.0014

Zhang, K., Zhang, P., Zhang, H., Tian, J., Wang, Z., and Xiao, J. (2024). Numerical simulation on sand sedimentation and erosion characteristics around HDPE sheet sand barrier under different wind angles. *J. Mt. Sci.* 21, 538–554. doi:10.1007/s11629-023-8302-4

Zhang, L., Liu, C., Fayek, M., Wu, B., Lei, K., Cun, X., et al. (2017). Hydrothermal mineralization in the sandstone–hosted hangjinqi uranium deposit, north ordos basin, China. *Ore Geol. Rev.* 80, 103–115. doi:10.1016/j.oregeorev.2016.06.012

Zhang, S., and He, Y. (2013). Analysis on the development and policy of solar PV power in China. *Renew. Sustain. Energy Rev.* 21, 393–401. doi:10.1016/j.rser.2013.01.002